



Article scientifique

Article

2013

Published version

Open Access

This is the published version of the publication, made available in accordance with the publisher's policy.

---

## Laser-induced condensation by ultrashort laser pulses at 248nm

---

Joly, Pierre; Petrarca, Massimo; Vogel, A.; Pohl, T.; Nagy, T.; Jusforgues, Q.; Simon, P.; Kasparian, Jérôme; Weber, K.; Wolf, Jean-Pierre

### How to cite

JOLY, Pierre et al. Laser-induced condensation by ultrashort laser pulses at 248nm. In: Applied physics letters, 2013, vol. 102, n° 9, p. 091112. doi: 10.1063/1.4794416

This publication URL: <https://archive-ouverte.unige.ch/unige:37060>

Publication DOI: [10.1063/1.4794416](https://doi.org/10.1063/1.4794416)



## Laser-induced condensation by ultrashort laser pulses at 248nm

P. Joly, M. Petrarca, A. Vogel, T. Pohl, T. Nagy, Q. Jusforgues, P. Simon, J. Kasparian, K. Weber, and J.-P. Wolf

Citation: [Applied Physics Letters](#) **102**, 091112 (2013); doi: 10.1063/1.4794416

View online: <http://dx.doi.org/10.1063/1.4794416>

View Table of Contents: <http://scitation.aip.org/content/aip/journal/apl/102/9?ver=pdfcov>

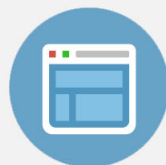
Published by the [AIP Publishing](#)

---



## Re-register for Table of Content Alerts

Create a profile.



Sign up today!



# Laser-induced condensation by ultrashort laser pulses at 248 nm

P. Joly,<sup>1</sup> M. Petrarca,<sup>1</sup> A. Vogel,<sup>2</sup> T. Pohl,<sup>2</sup> T. Nagy,<sup>3,4</sup> Q. Jusforgues,<sup>1</sup> P. Simon,<sup>3</sup> J. Kasparian,<sup>1,a)</sup> K. Weber,<sup>2</sup> and J.-P. Wolf<sup>1</sup>

<sup>1</sup>GAP-Biophotonics, Université de Genève, Chemin de Pinchat 22, 1211 Geneva 4, Switzerland

<sup>2</sup>Department of Mechanical and Process Engineering, Environmental Measurement Techniques, University of Applied Sciences, Düsseldorf, Josef-Gockeln-Str. 9, D-40474 Düsseldorf, Germany

<sup>3</sup>Laser-Laboratorium Göttingen e.V., Hans-Adolf-Krebs-Weg 1, 37077 Göttingen, Germany

<sup>4</sup>Institut für Quantenoptik, Leibniz Universität Hannover, Welfengarten 1, 30167 Hannover, Germany

(Received 17 October 2012; accepted 21 February 2013; published online 7 March 2013)

We compare laser-induced condensation by UV laser pulses of femtosecond, sub-picosecond, and nanosecond duration between each other, as well as with respect to near-infrared (NIR) (800 nm) ultrashort laser pulses. Particle nucleation by UV pulses is so efficient that their growth beyond several hundreds of nm is limited by the local concentration of water vapour molecules. Furthermore, we evidence a dual mechanism: While condensation induced by ultrashort UV pulses rely on nitrogen photo-oxidative chemistry like in the NIR, nanosecond laser-induced condensation occurs without NO<sub>2</sub> production, evidencing the domination of a mechanism distinct from that previously identified in the femtosecond regime. © 2013 American Institute of Physics. [<http://dx.doi.org/10.1063/1.4794416>]

Particle condensation by laser pulses attracts a strong interest<sup>1–4</sup> because of its potential implications in weather modulation, remote sensing of the atmospheric conditions, as well as information it may bear about the physico-chemistry of particle nucleation.<sup>5</sup> In the case of near-infrared (NIR) pulses, it relies on self-guided laser filaments,<sup>6–8</sup> a propagation mode typical of ultra-intense laser pulses in which a dynamic balance establishes between Kerr self-focusing and higher-order negative nonlinear contributions to the refractive index, namely ionization and/or the inversion of the Kerr effect.<sup>9,10</sup> The main mechanism behind NIR filament-induced condensation relies on the multiphoton-excited photochemical activation of the filament-generated plasma, resulting in the formation of ppm-range concentrations of hygroscopic HNO<sub>3</sub>,<sup>11</sup> the solvation of which thermodynamically stabilizes the growing particles.<sup>12</sup>

Up to now, experiments on laser-induced condensation have mostly focused on laser pulses at 800 nm, by far the most widely available spectral range because of a more mature laser technology. However, ultraviolet pulses can also induce filamentation.<sup>13</sup> Furthermore, short wavelengths are favourable to multiphoton processes, which require 3 to 4 times less photons in the UV than in the NIR (e.g., 2 photons to photo-excite molecular oxygen, ultimately yielding ozone), allowing much higher cross sections.<sup>14,15</sup> Indeed, continuous-wave UV light with a power as low as 7 W was shown to induce particle nucleation in humid conditions.<sup>16,17</sup> Very recently, the same authors extended their work to pulsed excimer laser up to the sub-Joule level (0.8 J, ≤100 MW), evidencing the growth of the nanoparticle size distribution over up to 30 min as the result of water condensation assisted by photochemically generated H<sub>2</sub>O<sub>2</sub>.<sup>4</sup> By offering an intensity typically 4 orders of magnitude higher,<sup>18,19</sup> focused, or filamenting ultrashort UV laser pulses can be expected to offer a much more efficient activation of nucleation and growth in the atmosphere.

Here, we compare the respective efficiencies of laser-induced condensation in air by state-of-the-art femtosecond, sub-picosecond, and nanosecond UV laser pulses. While the nanoparticle yields are rather similar for merely comparable incident peak powers, they lie typically one order of magnitude above the most powerful (3 J, ~100 TW) near-infrared pulses available to date. Finally, we discuss the implications for real-conditions experiments on a large scale.

As sketched in Figure 1, ultrashort UV (248 nm) laser pulses<sup>20</sup> generated by a home-built chirped-pulse amplification laser system<sup>21</sup> are focused from an initial diameter of 3 cm with a  $f=4$  m, into an open cloud chamber. Given the complex beam profile, the focal region in the chamber had a typical diameter of 1.5 mm. Pulses at a repetition rate of 5 Hz were emitted either uncompressed from the exit of the main excimer amplifier (25 mJ and 700 fs), or recompressed at the cost of an almost 2.5-fold loss in pulse energy (11 mJ and 110 fs). In each case, the laser energy was varied by attenuating the beam using a tilted dichroic mirror. Comparison measurements were performed with larger  $f$ -numbers, by using a  $f=10$  m lens as well as a collimated (unfocused) beam. Furthermore, we also investigated the effect of 20 ns long pulses of 320 mJ energy from an excimer laser in the same conditions.

The cloud chamber, similar to that described in Ref. 22, had an inner volume of  $58.8 \times 93.6 \times 69.6$  cm<sup>3</sup>. It was thermally isolated on its inner side with polystyrene (Jackodur KF 300) foam. An upward-pointing temperature gradient was maintained in the chamber by a liquid nitrogen reservoir on the bottom, separated from the main chamber volume by a 1 mm-thick steel plate. The inner chamber temperature and relative humidity (RH) in the vicinity of the laser beam were stabilized to  $15 \pm 1$  °C and  $92\% \pm 3\%$ , respectively, over the 3 min of each measurement.

The aerosol concentration between 2 cm and 5 cm distance from the laser beam side was monitored simultaneously by an aerosol spectrometers (Grimm, 1.109, 31 size classes from 250 nm to 32 μm, 6 s temporal resolution), each

<sup>a)</sup>E-mail: jerome.kasparian@unige.ch.

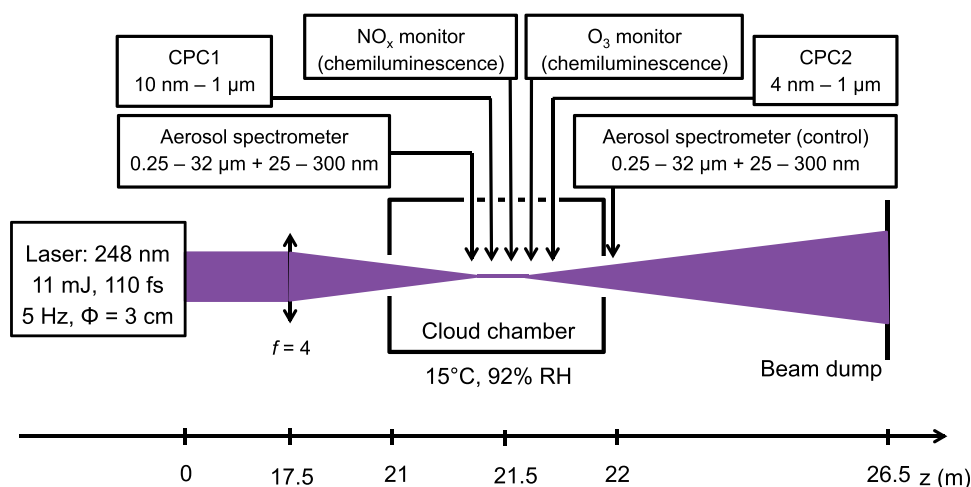


FIG. 1. Experimental setup. Grimm 1 and 2, TSI 4 nm, and TSI 10 nm are particles counters.

equipped with a nanoparticle detector (Grimm Nanocheck, 25–300 nm range in one single channel, and 10 s resolution). Control measurements were continuously performed by an identical aerosol spectrometer at the chamber exit to exclude any contamination of the measurement by transport of particles from outside of the chamber. The measurements were cross-checked with two condensation particle counters (CPC, TSI 3007 and 3775, offering measurement ranges 10 nm–1  $\mu\text{m}$ , and 4 nm–1  $\mu\text{m}$ , respectively). Simultaneously, the production of ozone and  $\text{NO}_x$  trace gases was monitored by chemiluminescence of organic dyes<sup>23</sup> and luminol,<sup>24</sup> respectively.

Launching the ultrashort UV laser into the cloud chamber results in the rise of the nano- as well as the micro-particle concentration within less than 1 min. For 10 mJ, 110 fs pulses, the rise reaches up to  $300\,000\text{ cm}^{-3}$  (i.e., 100 times the background concentration) after 3 min (900 pulses) for the 25–300 nm particles, with a measured median diameter of 40 nm. The increase still amounts to  $100\text{ cm}^{-3}$ , 7% of the background level, for  $0.43\text{ }\mu\text{m}$  particles. A direct quantitative comparison with our previous measurements in the NIR<sup>2,23</sup> is difficult because of the local fluctuations due to the air turbulence around the sampling region, as well as laser fluctuations between two experiments. Furthermore, the present experimental conditions were slightly different from the ones previously performed in the NIR, in terms of geometry, temperature, and relative humidity. Therefore, we can only estimate that the effect was 5–10 times larger than when using 10 000 times more powerful NIR pulses (3 J and 100 TW). This ratio is even more remarkable when considering that it is obtained in spite of a repetition rate of 5 Hz (as compared to 10 Hz in the NIR experiments), and that the sampling distance had to be increased in the present work in order to avoid saturation of the aerosol detectors dynamic range. These semi-quantitative arguments clearly evidence the much higher efficiency of UV ultrashort pulses for particle generation, as compared to NIR ones. This higher efficiency stems from the higher photon energy, resulting in lower-order non-linearity.

Consistent with the expectation of a lower-order process, the nanoparticle formation as well as the production of  $\text{NO}_2$  and ozone depend almost linearly on the input pulse energy (Figures 2(a) and 2(b)), in contrast to the strongly non-linear

behavior observed in the NIR.<sup>23,25</sup> In contrast, larger particles (see 265 nm particles in Figure 2(a) and mass-integrated measurements in Figure 2(c)) increase little, and even tend to decrease with increasing incident power over the investigated energy range. Simultaneously, the total condensed mass of particles up to  $1\text{ }\mu\text{m}$  increases slightly, but this increase is independent from the incident energy, while the total condensed mass of larger particles (up to  $10\text{ }\mu\text{m}$ ) tends to decrease for increasing energies (Figure 2(c)).

The contrast between the respective behaviors of the smaller and larger particles can appear counter-intuitive at a first glance. It can however be understood by considering that the particle growth is diffusion-limited, as was observed

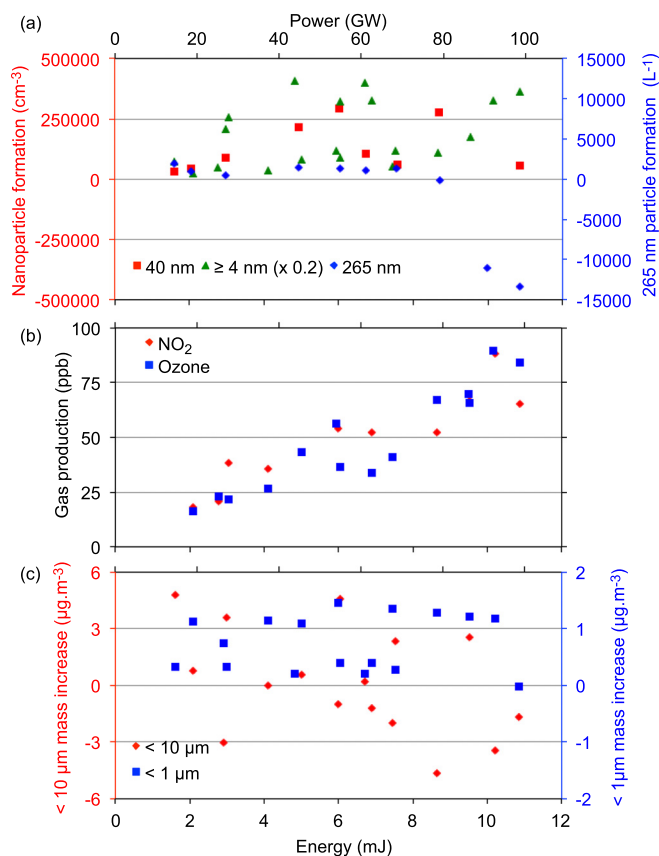


FIG. 2. Energy dependence of laser-induced formation of (a) nanoparticles (b) trace gases, and (c) condensed mass by 110 fs UV pulses at 248 nm.

in the case of NIR pulses the free atmosphere.<sup>2</sup> The transport towards the growing particles by diffusion of gas-phase water molecules available to condense is slow, so that at the 3-min timescale of the experiment, condensation is mainly restricted to the available stock of water vapour molecules (hence, controlled by the volume mixing ratio, VMR) in the atmosphere volume immediately surrounding the beam. Increasing the incident pulse, energy, hence the density of condensation nuclei available after the laser has been shot, induces a competition among these nuclei to harvest the available water vapor, thus limiting their growth, and consequently the concentration of larger particles. Sub-picosecond pulses (25 mJ and 700 fs), which feature a comparable incident energy and a peak power in the same range, offer a similar behaviour, as displayed in Figure 3.

The production of ozone and NO<sub>2</sub> by the ultrashort UV laser pulses suggests that the mechanism by which they induce condensation is similar to that reported in the NIR, based on multiphoton oxidative photo-chemistry of nitrogen, resulting in hygroscopic HNO<sub>3</sub> stabilizing the growing particles.<sup>2,12</sup> The corresponding remaining non-linearity of this process is evidenced by considering the effect of the beam focusing (Figure 4). While the efficiency of a fully linear process would be independent on focusing, we find that a tight focusing ( $f=4$  m) strongly increases the yield of UV femtosecond pulses on particle formation, again evidencing the influence of the input intensity. A loose focusing ( $f=10$  m) and a collimated beam are 1.5 and 100 times less efficient, respectively, in nanoparticle production at a moderate energy up to a few tens of mJ.

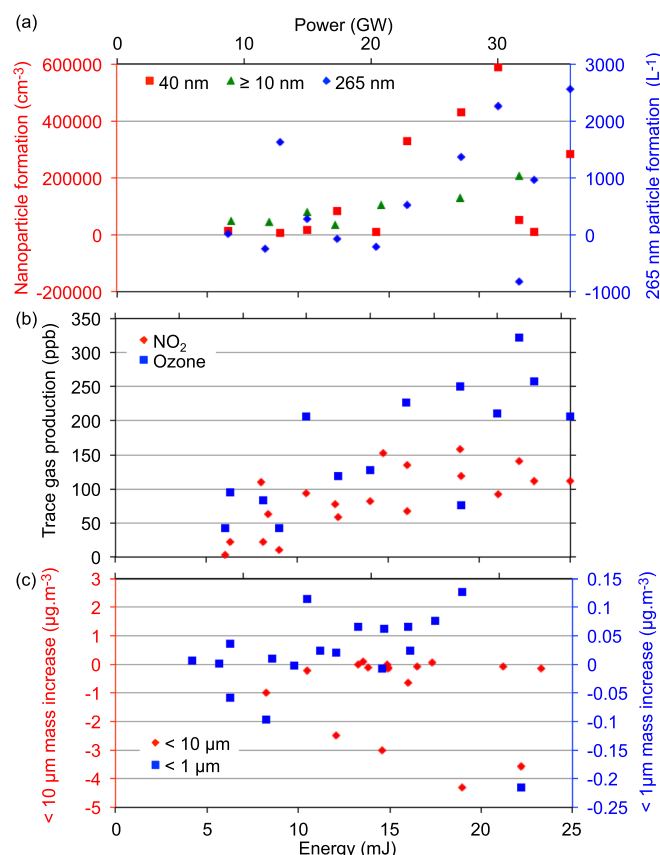


FIG. 3. Energy dependence of laser-induced formation of (a) nanoparticles, (b) trace gases, and (c) condensed mass by 700 fs UV pulses at 248 nm.

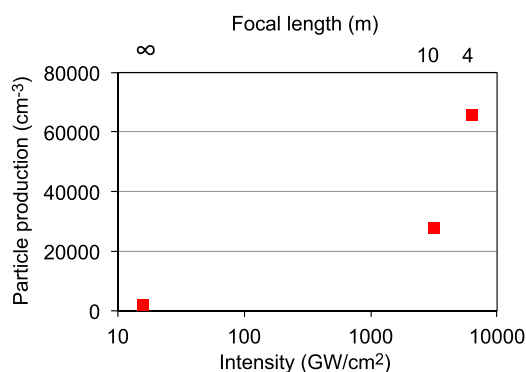


FIG. 4. Influence of geometrical focusing on the laser-induced nanoparticle formation by 110 fs, 9.5 mJ, and 248 nm pulses.

This much higher condensation efficiency in tightly focused beams strongly contrasts with the behavior observed in the NIR, where a collimated beam activates a larger volume in the atmosphere due to multiple filamentation over a longer range and results in more efficient condensation.<sup>25</sup> It can be related to the difficulty to generate laser filaments in the UV.<sup>13</sup> Together with the strong Rayleigh scattering, this finding underlines the need for further evaluation of the applicability of UV pulses to induce condensation over long ranges in the atmosphere: In spite of the higher particle yield, the spatial extension of the activated volume is much shorter.

The effect of ultrashort (fs and sub-ps) UV pulses contrasts with that of much longer pulses (20 ns) of moderate energy (up to 350 mJ). As displayed in Figure 5(a), the

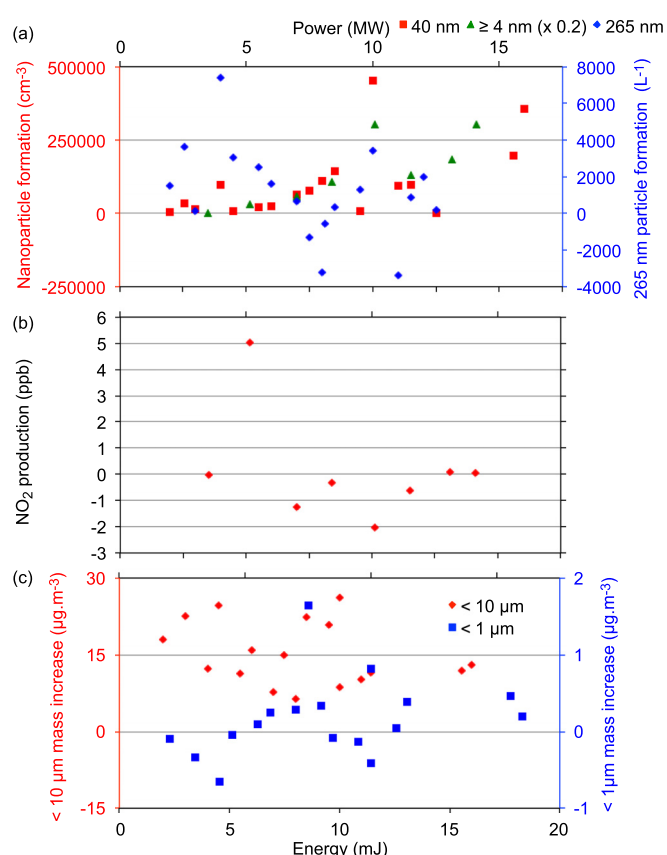


FIG. 5. Energy dependence of laser-induced formation of (a) nanoparticles, (b) trace gases, and (c) condensed mass by 20 ns UV pulses at 248 nm.



nucleation of particles in this case increases linearly with the input energy, consistent with the low incident power ( $\leq 15$  MW) and intensity ( $\leq 30$  MW/cm<sup>2</sup>). However, the net increase of condensed mass is limited to larger particles (up to 10  $\mu$ m, see Figure 5(c)), a behavior opposite to the short pulse case. We attribute this more efficient particle growth to the larger active volume in the case of nanosecond pulses. While self-focusing of femtosecond pulses tends to restrict the active volume to the narrow focal region, the nanosecond pulses offer a much wider and more homogeneous waist. This larger volume maximizes the amount of water molecules in the gas phase, available for condensation feeding the particle growth.

Furthermore, in contrast to the case of ultrashort pulses, condensation by nanosecond pulses is not accompanied by production of NO<sub>2</sub> (Figure 5(b)), clearly indicating a different photochemical pathway, which may imply on the photo-oxidation of volatile organic compounds and/or hydrogen peroxide, as recently proposed in similar experimental conditions.<sup>4</sup> The latter, which only needs one-photon excitation, depends linearly on the incident energy and would therefore dominate at low power, while multiphoton phenomena like that relying on HNO<sub>3</sub> (Refs. 2 and 12) would be more efficient in shorter pulses and higher intensities.

As a conclusion, we have observed the formation of nano- and micro-particles induced by UV laser pulses, in the femtosecond, sub-picosecond, as well as nanosecond regimes. The effect of ultrashort pulses appears to rely on a nitrogen-based process comparable to that evidenced in the case of NIR pulses, while VOC photo-oxidation and/or hydrogen peroxide production<sup>4</sup> offer a one-photon excited pathway dominating in the case of nanosecond pulses. The much higher condensation efficiency as compared to 100–1000 times more powerful and energetic NIR pulses<sup>23</sup> stems from a  $\sim 3$  times higher energy per photon. Further work is in progress to assess the scalability of these results to the atmospheric scale.

We gratefully acknowledge Bruno Neiningner (ZHAW, Zurich, Switzerland) for lending us the NO<sub>x</sub> detection system and TSI Inc. for providing us with the fast nanoscale particle systems. This work was supported by the European Research Council Advanced Grant “Filatmo.”

- <sup>1</sup>P. Rohwetter, J. Kasparian, K. Stelmaszczyk, Z. Hao, S. Henin, N. Lascoux, W. M. Nakaema, Y. Petit, M. Queißer, R. Salamé, E. Salmon, L. Wöste, and J.-P. Wolf, *Nat. Photonics* **4**, 451 (2010).
- <sup>2</sup>S. Henin, Y. Petit, P. Rohwetter, K. Stelmaszczyk, Z. Hao, W. Nakaema, A. Vogel, T. Pohl, F. Schneider, J. Kasparian, K. Weber, L. Wöste, and J.-P. Wolf, *Nat. Commun.* **2**, 456 (2011).
- <sup>3</sup>J. Ju, J. Liu, C. Wang, H. Sun, W. Wang, X. Ge, C. Li, S. L. Chin, R. Li, and Z. Xu, *Opt. Lett.* **37**, 1214–1216 (2012).
- <sup>4</sup>K. Yoshihara, Y. Takatori, and Y. Kajii, *Bull. Chem. Soc. Jpn.* **85**, 1155–1159 (2012).
- <sup>5</sup>J. Kasparian, P. Rohwetter, L. Wöste, and J.-P. Wolf, *J. Phys.D: Appl. Phys.* **45**, 293001 (2012).
- <sup>6</sup>A. Couaïron and A. Mysyrowicz, *Phys. Rep.* **441**, 47–189 (2007).
- <sup>7</sup>L. Bergé, S. Skupin, R. Nuter, J. Kasparian, and J.-P. Wolf, *Rep. Prog. Phys.* **70**, 1633–1713 (2007).
- <sup>8</sup>S. L. Chin, S. A. Hosseini, W. Liu, Q. Luo, F. Théberge, N. Aközbek, A. Becker, V. P. Kandidov, O. G. Kosareva, and H. Schröder, *Can. J. Phys.* **83**, 863–905 (2005).
- <sup>9</sup>P. Béjot, J. Kasparian, S. Henin, V. Loriot, T. Vieillard, E. Hertz, O. Faucher, B. Lavorel, and J.-P. Wolf, *Phys. Rev. Lett.* **104**, 103903 (2010).
- <sup>10</sup>P. Béjot, E. Hertz, B. Lavorel, J. Kasparian, J.-P. Wolf, and O. Faucher, *Phys. Rev. Lett.* **106**, 243902 (2011).
- <sup>11</sup>Y. Petit, S. Henin, J. Kasparian, and J.-P. Wolf, *Appl. Phys. Lett.* **97**, 021108 (2010).
- <sup>12</sup>P. Rohwetter, J. Kasparian, L. Wöste, and J.-P. Wolf, *J. Chem. Phys.* **135**, 134703–134703-6 (2011).
- <sup>13</sup>J. Schwarz, P. Rambo, and J.-C. Diels, *Opt. Commun.* **180**, 383–390 (2000).
- <sup>14</sup>A. Sorokin and F. Arnold, *Atmos. Environ.* **43**, 3799–3807 (2009).
- <sup>15</sup>A. Sorokin, *Atmos. Chem. Phys.* **10**, 3141–3145 (2010).
- <sup>16</sup>K. Yoshihara, *Chem. Lett.* **34**, 1370 (2005).
- <sup>17</sup>K. Yoshihara, Y. Takatori, K. Miyazaki, and Y. Kajii, *Proc. Jpn. Acad. Ser. B* **83**, 320–325 (2007).
- <sup>18</sup>J. Kasparian, R. Sauerbrey, and S. L. Chin, *Appl. Phys. B* **71**, 877–879 (2000).
- <sup>19</sup>A. Becker, N. Aközbek, K. Vijayalakshmi, E. Oral, C. M. Bowden, and S. L. Chin, *Appl. Phys. B* **73**, 287–290 (2001).
- <sup>20</sup>T. Nagy and P. Simon, *Opt. Express* **17**, 8144 (2009).
- <sup>21</sup>G. Marowsky, P. Simon, K. Mann, and C. K. Rhodes, in *Springer Handbook of Lasers and Optics*, 2nd ed., edited by F. Träger (Springer, Berlin, 2012), Chap. 11.7, pp. 832–852.
- <sup>22</sup>M. Petrarca, S. Henin, K. Stelmaszczyk, S. Bock, S. Kraft, U. Schramm, C. Vanep, A. Vogel, J. Kasparian, R. Sauerbrey, K. Weber, L. Wöste, and J.-P. Wolf, *Appl. Phys. Lett.* **99**, 141103–141103-3 (2011).
- <sup>23</sup>A. Zahn, J. Weppner, H. Widmann, K. Schlote-Holubek, B. Burger, T. Kühner, and H. Franke, *Atmos. Meas. Technol.* **5**, 363–375 (2012).
- <sup>24</sup>Swiss Agency for the Environment, Forests and Landscape, *Environmental Documentation No. 111 (Air)*, edited by J. Dommen, A. S. H. Prévôt, B. Neiningner, N. Clark, B. Neiningner, M. Baumle, M. Lehning, and O. Liechti (1999), p. 119.
- <sup>25</sup>Y. Petit, S. Henin, J. Kasparian, J. P. Wolf, P. Rohwetter, K. Stelmaszczyk, Z. Q. Hao, W. M. Nakaema, L. Wöste, A. Vogel, T. Pohl, and K. Weber, *Appl. Phys. Lett.* **98**, 041105 (2011).